Nanophotothermolysis of multiple scattered cancer cells with carbon nanotubes guided by time-resolved infrared thermal imaging

Alexandru S. Biris
University of Arkansas at Little Rock
Applied Science Department
Nanotechnology Center
Little Rock, Arkansas 72204

Dorin Boldor
Jason Palmer
William T. Monroe
Louisiana State University Agricultural Center
Department of Biological and Agricultural Engineering
Baton Rouge, Louisiana 70803

Meena Mahmood
Enkeleda Dervishi
Yang Xu
Zhongrui Li
University of Arkansas at Little Rock
Applied Science Department
Nanotechnology Center
Little Rock, Arkansas 72204

Ekaterina I. Galanzha
Vladimir P. Zharov
University of Arkansas for Medical Sciences
Philips Classic Laser and Nanomedicine Laboratories
Little Rock, Arkansas 72205

Abstract. Nanophotothermolysis with long laser pulses for treatment of scattered cancer cells and their clusters is introduced with the main focus on real-time monitoring of temperature dynamics inside and around individual cancer cells labeled with carbon nanotubes. This technique utilizes advanced time- and spatially-resolved thermal radiometry imaging for the visualization of laser-induced temperature distribution in multiple-point absorbing targets. The capability of this approach was demonstrated for monitoring of thermal effects under long laser exposure (from millisecond to seconds, wavelength 1064 nm, maximum power 1 W) of cervical cancer HeLa cells labeled with carbon nanotubes *in vitro*. The applications are discussed with a focus on the nanophotothermolysis of small tumors, tumor margins, or micrometastases under the guidance of near-IR and microwave radiometry.
[DOI: 10.1117/1.3119135]

Keywords: nanophotothermolysis; nanoparticles; photothermal radiometry; cancer; carbon nanotubes.

Paper 08323SSR received Sep. 9, 2008; revised manuscript received Jan. 17, 2009; accepted for publication Feb. 14, 2009; published online Apr. 28, 2009.

Photothermal (PT) therapy of tumor cells tagged by various optically absorbing nanoparticles (NPs) is usually utilized in two main modes using short (e.g., nanosecond) laser pulses[1,2] or relatively long continuous (cw) laser exposure.[3,4] The first mode is more effective for the ablation of individual metastatic or residual cells by laser-inducement of microbubbles around overheated NPs and their clusters with local temperature increase to 150 to 300 °C. This can be achieved without harmful effects for the surrounding healthy cells because of the negligible heat dissipation during the application of short pulses and because of the highly localized (within a few micrometers) microbubbles present within and around the targeted cells.[5] Particularly, this method has significant potential for *in vivo* blood purging by ablating every single circulating tumor cells in the peripheral blood vessels under a single laser pulse.[6] The second mode requires at least a few minutes of laser cw exposure, producing cellular damage due to the thermal protein denaturation at temperature levels of 45 to 65 °C. This mode could be more appropriate for the treatment of primary tumors with relatively large sizes of a few and more millimeters, given its more effective heat redistribution through the whole tumor volume.

Surprisingly, there were no previous reports of using laser PT therapy for the treatment metastaic tumors, which cause up to 90% of all the cancer-related deaths. Both modes can be used with some limitations or at least precautions in the treatment of multiple scattered micrometastases or even single cancer cells. In the first mode, the high local thermal and bubble phenomena during the laser pulse application may partly attenuate the laser radiation due to the thermolens defocusing or scattering effects, while in the second mode, thermal diffusion during a long exposure can lead to damage of healthy tissues around the micrometastasis. Here we emphasize that an intermediate mode with long laser pulses can potentially overcome these disadvantages. The laser-induced moderate temperatures of around 80 to 95 °C are high enough to damage localized tumor cell clusters, while the short exposure time will not allow extensive heat dissipation and hence damage the healthy cells around these clusters.

The ability to control and monitor the temperature around targeted cells is very important for both PT modes and, espe-

Address all correspondence to: Alexandru Biris or Vladimir P. Zharov, Philips Classic Laser and Nanomedicine Laboratories, University of Arkansas for Medical Sciences, Little Rock, Arkansas 72205. Tel: 501-749-9148; Fax: 501-683-7601 E-mail: asbiris@ualr.edu or ZharovVladimirP@uams.edu.

1083-3668/2009/14(2)/021007/6/$25.00 © 2009 SPIE

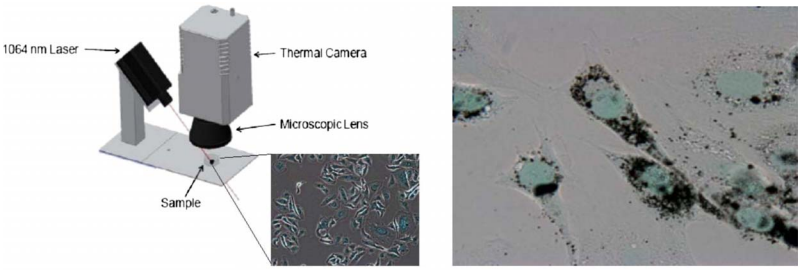

Fig. 1 (a) Schematic of PT radiometry for monitoring temperature distribution during PT cancer therapy *in vitro* and (b) the HeLa cells after the incubation for 48 h with CNTs.

cially, for this novel PT metastasis therapy that enables the successful inducement of cancer cell thermal damage with minimized collateral effects. Until now, various methods were used to measure laser-induced thermal effects around NPs including optical detection of temperature dependent variation of the refractive index,[1] magnetic resonance imaging[3] (MRI), and infrared (IR) radiometry.[5] However, to our knowledge, no published study exists that simultaneously determines the spatial and temporal temperature distribution at microscopic scale with high temporal and spatial resolution even *in vitro*. We demonstrate here that IR PT radiometry, broadly used before in laser medicine,[7,8] combined with recent advances in time-resolved IR imaging techniques, is a very useful tool for determining the temperature dynamics in scattered individual cancer cells or their small clusters labeled with carbon nanotubes (CNTs).

A cw laser (model DP-1064-1000K, Lasermate Group, Inc., Pomona, California) operating at 1064 nm was used to irradiate a monolayer of HeLa cells on a glass substrate after being incubated with CNTs for various periods of time (Fig. 1). The maximum power level of the laser is 1 W, controlled by a Newport Power Meter model 1815-C (Newport Corp., Irvine, California). The laser was located 15.5 cm away from the surface of the samples at a 45-deg angle. The angle of the beam and location of the laser were chosen to minimize interference with the microscopic lenses of the IR camera, and for the laser not to be placed in the optical path of the camera. The beam has a Gaussian distribution with a $1/e^2$ value of 2 mm at the aperture, resulting in a relatively smooth flat-intensity profile over a central circular area. The time-resolved IR thermal origin images of the samples were acquired at a rate of 60 Hz and recorded to a sequence file using a calibrated forward-looking IR (FLIR) A40 thermal camera (FLIR Systems, Inc., Boston, Massachusetts) and FLIR Thermacam Researcher software (FLIR Systems, Inc., Boston, Massachusetts). A FLIR Macro Lens (FLIR Systems, Inc., Boston, Massachusetts) was attached to the camera, resulting in a 17× fixed magnification and a field of view of approximately 4 ×6 mm. The camera has a maximum spatial resolution of 18 μm/pixel and temperature resolution of 0.07 °C. For data analysis, FLIR Thermacam Researcher sessions were embedded in Microsoft Excel (Microsoft Corp., Redmond, Washington).

Multiwalled CNTs were used as PT contrast agents,[4,9] and were synthesized[10,11] by radio-frequency chemical vapor deposition (rf-CVD) over a Fe-Co/$CaCO_3$ catalyst (2.5:2.5:95 wt%). About 100 mg of the catalyst was uniformly spread into a thin layer on a graphite susceptor and placed in the center of a quartz tube with inner diameter of 1 in. The quartz tube was horizontally positioned at the center of the rf generator. Next, the system was purged with nitrogen at 200 ml/min for 10 min, and when the temperature reached 720 °C, acetylene was introduced at 3.3 ml/min for 30 min. The as-produced CNTs were purified in one simple step using diluted hydrochloric acid solution and sonication.

As a model target, mammalian cervical cancer cells (HeLa cells) were seeded in 10-cm culture plates (0.5×10^6 cells/plate) with growth medium (minimum essential medium containing 10% fetal bovine serum and 1% penicillin 100 unit/ml, streptomycin 100 μg/ml) and incubated for 2 days using a humidified incubator (37 °C, 5% CO_2) for the stock culture. Cells were dissociated by 1× trypsin in phosphate-buffered saline (PBS) and counted and plated into 16 plates of 35-mm culture dishes at 5×10^4 cells/dish and supplemented by a growth medium with various concentrations of CNTs (0.83 to 20 μg/ml) and without CNTs for control (0 μg/ml Vehicle). Then the cells were dissociated from the bottom of the plate by 1× trypsin and transferred to 1.5 Eppendorf tubes and spun down. Finally, the viability of labeled and control cells was determined with the trypan blue test. We added 25 μl of 1× trypan blue dye to each sample and incubated for less than 5 min. The viable cell number was counted through a hemocytometer.

Thermogravimetric analysis (TGA) (Mettler Toledo TGA/SDTA 851e.) was performed to characterize the thermal behavior and purity of CNTs at an airflow of 150 ml/min. In this study, we wanted to use very pure CNTs with little or no other carbonaceous species or other metallic impurities, which would further change the outcome of this research. The TGA curve provides information about the thermal stability of CNTs, and the first derivative of this curve determines the maximum decomposition temperature of the sample. The normalized TGA analysis and its first derivative of the purified CNTs indicate a significant mass drop around 551 °C, which corresponds to the weight loss in the combustion of the CNTs. As long as laser-induced temperatures are lower than this critical value, CNTs would be extremely stable in the cell culture. The quantitative TGA revealed that after the single-step purification, the purity of the CNT product is higher than 98%.

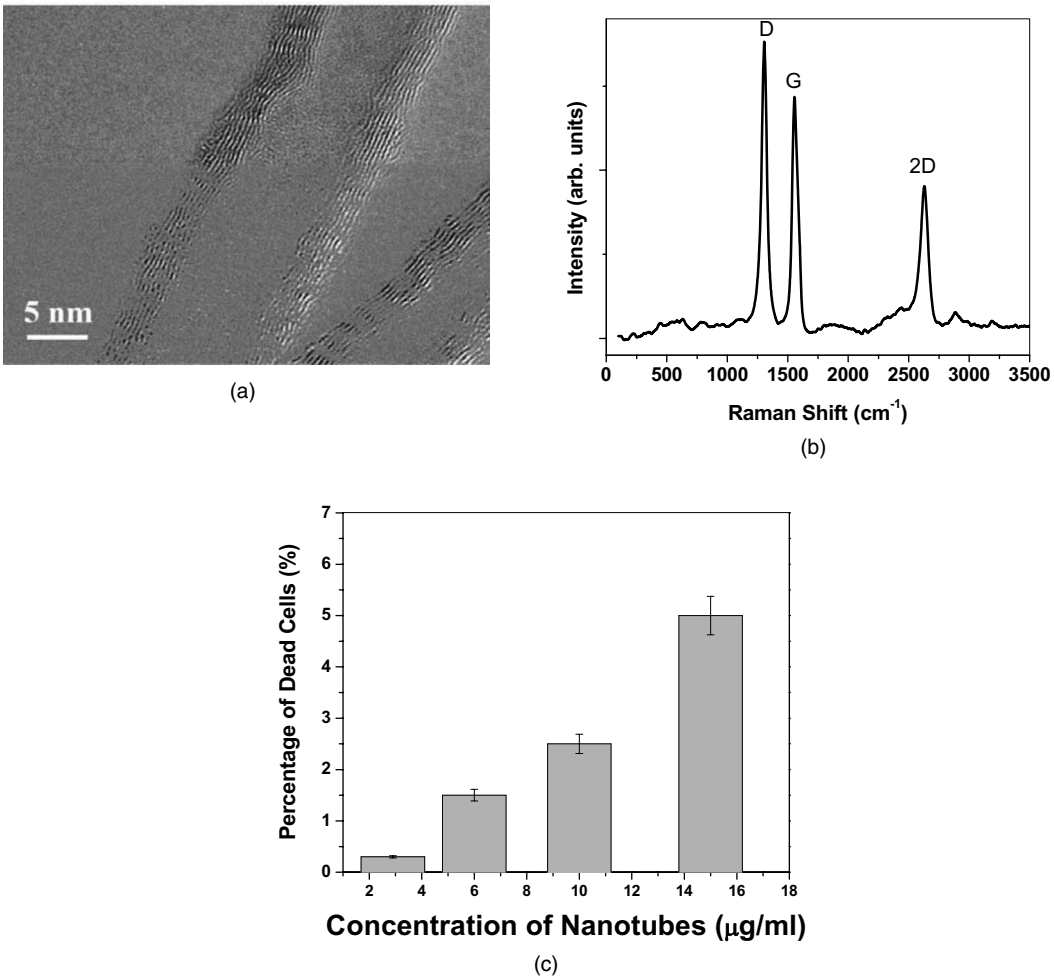

Fig. 2 High-resolution TEM image of multiwall CNTs (MWCNTs) grown over the Fe-Co/$CaCO_3$ catalyst, (b) Raman scattering spectra of the MWCNTs produced on the Fe-Co/$CaCO_3$ catalyst with acetylene as carbon source, and (c) cytotoxicity studies of the MWCNTs in the cervical cancer HeLa cells (48 h).

The morphology and quality of the CNTs [Fig. 2(a)] were thoroughly characterized by high-resolution transmission electron microscopy (TEM) (model JEOL 2100 FE, Boston, Massachusetts). Raman scattering spectroscopy of the CNTs grown on Fe-Co/$CaCO_3$ [Fig. 2(b)] was performed using Horiba Jobin Yvon LabRam HR800 equipped with a CCD, a spectrometer with grating of 600 lines/mm, and a He–Ne laser (633 nm, 20 mW) as an excitation source. The characteristics bands for CNTs are the D band, G band, and the 2D band.[12,13] The D band is present between 1305 and 1330 cm^{-1} and is related to the presence of defects and impurities in the CNTs. The G band present between 1500 and 1605 cm^{-1}, is also known as the tangential band and arises from the E_{2g} mode of the graphite plane. The G band position is relatively constant for the CNT material excited at different energies. The last important mode observed in the Raman spectrum of CNTs is the 2D band or the second-order harmonic of the D band, which is often present between 2450 and 2650 cm^{-1}.

It is known that CNTs have a high ability to penetrate and agglomerate inside of various cellular subcompartments.[4] Optical microscopy analysis confirmed that the CNTs were clustered inside the cells a few hours after CNT addition to the culture medium [Fig. 1(b)]. It can be observed that significant amounts of CNTs have penetrated the cellular membrane into the cytoplasm and in smaller quantities into the nucleus. There were no observable changes in the cell morphology due to the presence of CNTs. The CNT cytotoxic effects after their delivery into cells and tissues is still a subject of intense scientific debate.[14,15] In our study, the CNTs were not observed to have a major cytotoxic effect, as highlighted by Fig. 2(c). Even at relatively large CNT concentrations, only about 5% of the cells were necrotic relative to the control.

Advanced IR thermography with modern optical-electronic platforms was used for remote measuring the laser-induced PT effects with no spectral overlap in laser near-IR (NIR) excitation (1064 nm) and mid-IR thermal radiation[16] (band 7.5 to 13 μm). This process can be especially useful for studying the heating properties of graphitic structures, such as CNTs, which are known to absorb very strongly in the IR region and were shown to heat[16] to over 250 °C in less than 2 s.

The cells were exposed to the 1064-nm laser irradiation before and after the cells were incubated with CNTs for 48 h. No effects from the laser exposure was observed on the cells

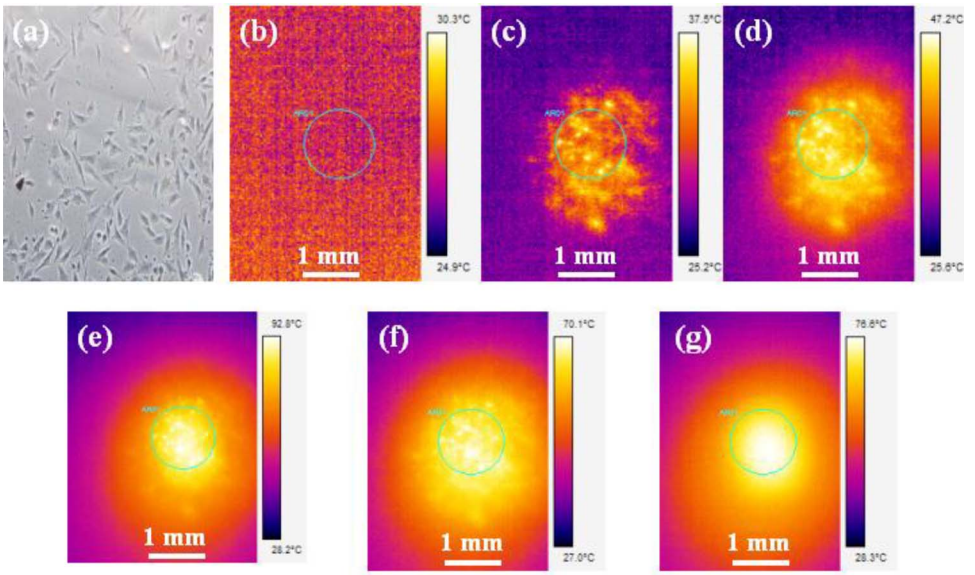

Fig. 3 Time-resolved PT radiometry imaging of temperature dynamic around cancer cells at various periods of time ("2-D temporal temperature mapping") during the cw laser exposure (wavelength, 1064 nm; power, 1 W; beam diameter, 2 mm at aperture): (a) optical image (image height, approx. 4.3 mm), and at various time (t) intervals during laser treatment; (b) $t=0$; (c) $t=0.2$ s; (d) $t=0.6$ s; (e) $t=1.2$ s; (f) $t=2.2$ s; and (g) $t=3.4$ s.

that did not contain CNTs. IR thermal analysis studies performed before the cells were incubated with CNTs indicated no notable temperature variation (less than 1.5 °C) induced by the laser radiation. These results can be explained by the relatively low absorption of the 1064-nm laser by the cellular compounds[7,8] (mainly water with a low coefficient of absorption of $\sim 0.1\ cm^{-1}$). The IR thermal images of cells incubated with CNTs and collected at various periods of time after the laser exposure are shown in Fig. 3. We can observe that immediately after the laser is turned on, local hot spots begin to develop [Fig. 3(c)]. These hot spots are associated with the near-instantaneous laser interaction and heating of individual and agglomerations of CNTs present inside the individual or clustered cancer cells. We can readily observe that there are multiple identical points in Figs. 3(b) and 3(c), such that the analysis of a single hot spot (the hottest spot) is extremely representative for the whole sample. This phenomenon is followed by a rapid heat redistribution from the CNTs due to the heat diffusion inside the cell compartments, leading to the heating of the whole cell. Further, the heat propagates from the individual cells to the surrounding intercellular liquid environment. In a relatively short period of time (approximately 2 s), the thermal spots of the individual cells are overlapping and as the time progresses, the dimensions of these hot spots gradually increase. Within 4 s [Fig. 3(d)], the entire volume exposed to the laser irradiation reaches the same temperature as the cells. Therefore, the hot spots observed initially represent individual cancer HeLa cells, and after less than 4 s it was observed that the temperature in the whole focal volume became relatively uniform. Finally, heat propagates out of the beam diameter. As an example, Fig. 4(a) shows the data collected from IR thermal images indicating the temperature variation as a function of time, inside of a single HeLa cell and at different distances away from the cells and/or beam. After 4 s, the laser was turned off and the temperature was found to decrease almost exponentially. The qualitative description of thermal dynamics in multiple absorbing targets such as cancer cells with CNTs are in line with theoretical models developed recently by us for multiple gold nanoparticles in an irradiated volume.[17] Since the laser radiation is highly absorbed by the individual CNTs, they are expected to heat up and create localized damage in various cellular subcompartments, which may induce necrosis. Since the heat capacity of the CNTs as compared to that of the solution is extremely small, the overall solution temperature increase is significantly slower (in seconds). After being incubated with the CNTs for 48 h, the overall heating process as a function of heating time of the cells was found to be mostly governed by a first-order exponential law, but a balance between the heat induced in the nanoparticles and the heat dissipated into the liquid environment of the cells and the external medium is reached in seconds. The heat transfer into the liquid medium is mostly of a linear nature and is dependent on the thermal capacity and properties of the liquid environments. According to the data presented in Fig. 4(a), only 3.8 s after the laser exposure, the temperature inside the cells increased to as much as 95 °C. Considering this extreme temperature, it is virtually guaranteed that all cells in the area become necrotic, as it has been shown that temperatures of 62 °C ensure the thermal ablation of human cells during this time scale.[18] The difference between this measured temperature inside individual cells and the values measured earlier for powdered nanotubes[16] can be attributed to the laser energy absorbed by the liquid environment around the cells and the smaller amount of CNTs present inside of the individual cells. The best mathematical equation that describes the time-temperature relationship was found to be given by the first-order equation: $T=a+b(1-e^{-ct})$, where a (initial temperature), b (amplitude of final response), and $1/c$ (time constant) are constants that depend on the specific experimental conditions.

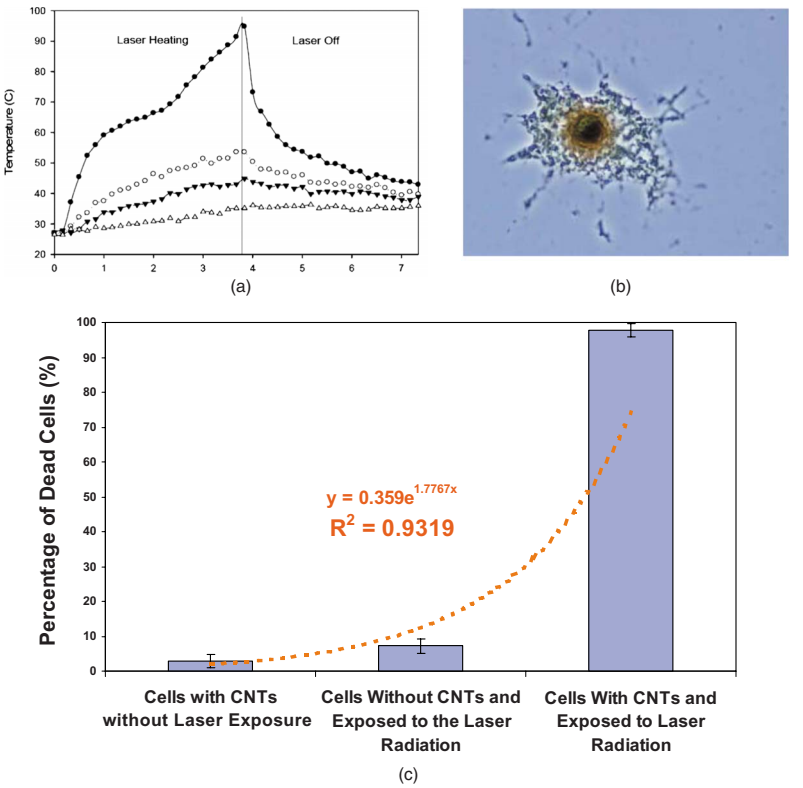

Fig. 4 Relationship between the temperature inside and outside the cells at various distances as a function of the irradiation time. The curves from top to bottom represent the temperature inside the laser beam (filled circles), at the outer edge of the beam (hollow circles), 1 (filled triangles), and 2 mm away from the beam (hollow triangles). (b) Completely disintegration of single cell with CNTs (48-h incubation) due to the heating process induced by laser exposure (1064 nm, ~31 W/cm^2, 1 W, 4 s). The measurements were performed in identical conditions. (c) Percentage of HeLa cells (with and without CNTs) that died under laser irradiation (4 s).

Based on this equation, the maximum temperature attainable in the studied experimental conditions at a steady state will be 114 °C (initial value plus final response). The time constant is only 3.125 s, indicating the speed with which the CNT/cells/medium mixture reacts to the laser stimulation. By comparison, we have previously shown[16] that the time constant of raw CNTs response to the same wavelength laser radiation is approximately 1.25 s. As the distance away from the cells increases, the temperature=time relationship was found to become a linear one, which is mostly governed by the thermal diffusion inside the liquid medium and the density of cells that contain CNTs, as shown in Fig. 4(a).

The heating level and rate of the cells tagged with CNTs is governed by the heating properties of the CNTs. The thermal properties of CNTs, including their specific heat, thermal conductivity, and thermo power, strongly depend on the phonon dispersion relations and the phonon density of states. The dominant contribution to the heat capacity comes from the phonons, while the electronic contribution can be essentially neglected. Each CNT is excited to the electronic excited state, followed by a rapid relaxation to the ground state with an effective electron-phonon conversion of the absorbed photon energy into thermal energy. Due to the fast heat diffusion time, thermal energy rapidly diffuses along the CNT wall and then to the medium inside and outside of the wall. Thus, the laser radiation simultaneously heats most of the multiple absorbing carbon layers of the nanotubes and most of the individual and clustered CNTs. Overall heat generated will be directly proportional to the amount of CNTs that are present inside the focal volume of the laser. An interesting observation is that even at millisecond exposure times, the temperature inside the cells becomes over 50 to 60 °C (i. e., protein denaturation threshold), indicating the possibility of killing the cells at appropriate laser irradiation of short duration. After only several seconds of laser irradiation, temperature differences of as high as 70 °C were recorded inside of the cells that were incubated with the CNTs as compared with the control. These results prove the high laser absorption properties of the CNTs and their role in inducing heat inside of the cells. After the laser irradiation process, the cells were found to completely disintegrate during just 4 s due to the heating process [Fig. 4(b)]. Figure 4(c) shows the percentage of cells that died under the laser exposure (4 s) without and with CNTs (10 μg/ml). When cells that were incubated with CNTs were exposed to the laser radiation, in a short time, around 98% of them died due to the temperature induced by the internalized nanotubes under the laser irradiation.

The importance of validating the temperature kinetics during PT therapy for individual cancer cells *in vitro* cannot be overlooked, as the dosing regimens are extremely important when moving toward *in vivo* studies. It is generally known that laser PT therapy (without thermal absorbers such as CNTs) is used in several conditions, especially for skin tissue. However, overexposure to radiation used in treatment of subcutaneous legions (or even for recreational and cosmetic pur-

poses such as tanning) can lead to unwanted side effects due to the higher dosage required to compensate for the scattering occurring on the transmission pathway through the skin and subcutaneous tissue. The detailed and accurate knowledge of temperature kinetics of CNT-loaded cancerous cells exposed to electromagnetic stimulation is therefore critical in determining the appropriate dose regimens for laser PT therapy using relatively long laser pulses or other electromagnetic stimulations of cancer cells circulating in the microvessels at various depths in the tissue. The side effects due to overexposure can be minimized or even eliminated, especially in the context of the simultaneous detection of the CNT-labeled cancer cells just prior to turning the laser on. As the cells heat up extremely fast, the total exposure can be limited to several seconds at a time, during which a high enough quantity of cells are heated in the vicinity of the CNT-labeled ones, such as the risk of recovery from a neighboring cancer cell that would not be treated with a pulsed laser is minimized.

In summary, we demonstrated the utility of the advanced PT image radiometry for time- and space-resolved monitoring of laser heating of individual cancer cells labeled by CNTs (i.e., nanophotothermolysis at single cells level.[1,2]) The cytotoxicity of the CNTs was found to be relatively low with a value of 5% at maximum CNT loading. After the laser exposure, the temperature inside the cells was found to reach values as high as 95 °C, enough to induce localized damage and ultimately cell necrosis. The temperature increase inside the cells was found to have a nonlinear first-order behavior, which can be explained by the combination of laser-induced temperature dynamics into individual cells and subsequent heat transfer among neighboring individual cells within laser beam. Thus, we introduce the experimental verification of temporal and spatial temperature kinetics at the microscale during laser-based nanophotothermolysis of multiple cancer cells and small cell clusters scattered in the irradiated volume. Such a method could prove to be extremely useful for the optimization of laser PT therapy *in vitro* and development of real-time, laser-based detection methods of cancer cells and their simultaneous killing during the detection process using a combination of IR with microwave, and near-IR radiometry which provide assessment for both surface and deep (up to 3 cm) temperature in tissue.[19,20]

Acknowledgments

This work was supported in part by the National Institute of Health under Grant Nos. EB600873, EB005123, and CA131164, and by the Arkansas Bioscience Institute.

References

1. V. Zharov, V. Galitovsky, and M. Viegas, "Photothermal detection of local thermal effects during selective nanophotothermolysis," *Appl. Phys. Lett.* **83**(24), 4897–4899 (2003).
2. E. K. Joe, X. Wei, R. R. Anderson, and C. P. Lin, "Selective cell targeting with light-absorbing microparticles and nanoparticles," *Biophys. J.* **84**, 4023–4032 (2003).
3. L. R. Hirsch, R. J. Stafford, J. A. Bankson, S. R. Sershen, B. Rivera, R. E. Price, J. D. Hazle, N. J. Halas, and J. L. West, "Nanoshell-mediated near-infrared thermal therapy of tumors under magnetic resonance guidance," *Proc. Natl. Acad. Sci. U.S.A.* **100**(23), 13549–13554 (2003).
4. N. W. S. Kam, M. O'Connell, J. A. Wisdom, and H. Dai, "Carbon nanotubes as multifunctional biological transporters and near-infrared agents for selective cancer cell destruction," *Proc. Natl. Acad. Sci. U.S.A.* **102**, 11600–11605 (2005).
5. V. P. Zharov, E. N. Galitovskaya, C. Jonson, and T. Kelly, "Synergistic enhancement of selective nanophotothermolysis with gold nanoclusters: potential for cancer therapy," *Lasers Surg. Med.* **37**, 219–226 (2005).
6. V. Zharov, E. Galanzha, E. Shashkov, I. Maksimova, B. Khlebtsov, N. Khlebsov, G. Terentuk, G. Akchurin, and V. Tuchin, "*In vivo* detection and killing of individual circulating metastatic cells," *Lasers Surg. Med.* **19**, 47–48 (2007).
7. A. M. Prokhorov, G. P. Chebotareva, and V. P. Zharov, "Pulsed photothermal radiometry of bioobjects with CO_2, Nd:YAG and Er; YAG lasers," *IEEE J. Quantum Electron.* **16**, 1981–989 (1989).
8. I. A. Vitkin, B. C. Vilson, and R. R. Anderson, "Pulsed photothermal radiometry studies in tissue optics," in *Optical-Thermal Response of Laser-Irradiated Tissue*, A. J. Welch and M. J. C. van Gemert, Eds., pp. 535–560, Plenum Press, New York (1995).
9. J. W. Kim, E. I. Galanzha, E. V. Shashkov, N. Kotagiri, and V. P. Zharov, "Photothermal antimicrobial nanotherapy and nanodiagnostics with self-assembling carbon nanotube clusters," *Lasers Surg. Med.* **39**, 622–634 (2007).
10. E. Dervishi, Z. Li, A. R. Biris, D. Lupu, S. Trigwell, and A. S. Biris, "Morphology of multi-walled carbon nanotubes affected by the thermal stability of the catalyst system," *Chem. Mater.* **19**(2), 179–184 (2007).
11. E. Couteau, K. Hernadi, J. W. Seo, L. Thien-Nga, C. S. Miko, R. Gaal, and L. Forro, "CVD synthesis of high-purity multiwalled carbon nanotubes using $CaCO_3$ catalyst support for large-scale production," *Chem. Phys. Lett.* **378**, 9–17 (2003).
12. M. S. Dresselhaus, G. Dresselhaus, A. Jorio, A. G. Souza Filho, and R. Saito, "Raman spectroscopy on isolated single wall carbon nanotubes," *Carbon* **40**(12), 2043–2061 (2002).
13. M. S. Dresselhaus, G. Dresselhaus, R. Saito, and A. Jorio, "Raman spectroscopy of carbon nanotubes," *Phys. Rep.* **409**, 47–99 (2005).
14. C. A. Poland, R. Duffin, I. Kinloch, A. Maynard, W. A. H. Wallace, A. Seaton, V. Stone, S. Brown, W. MacNee, and K. Donaldson, "Carbon nanotubes introduced into the abdominal cavity of mice show asbestos-like pathogenicity in a pilot study," *Nat. Nanotechnol.* **3**(7), 423–428 (2008).
15. M. L. Schipper, N. Nakayama-Ratchford, C. R. Davis, N. Wong Shi Kam, P. Chu, Z. Liu, X. Sun, H. Dai, and S. S. Gambhir, "A pilot toxicology study of single-walled carbon nanotubes in a small sample of mice," *Nat. Nanotechnol.* **3**, 216–221 (2008).
16. D. Boldor, N. M. Gerbo, W. T. Monroe, J. H. Palmer, Z. Li, and A. S. Biris, "Temperature measurement of carbon nanotubes using infrared thermography," *Chem. Mater.* **20**(12), 4011–4016 (2008).
17. A. V. Brusnichkin, D. A. Nedosekin, M. A. Proskurnin, and V. P. Zharov, "Photothermal lens detection of gold nanoparticles," *Appl. Spectrosc.* **61**, 1191–1201 (2007).
18. T. G. Barton, H. J. Foth, M. Christ, and K. Hormann, "Interaction of holmium laser radiation and cortical bone: ablation and thermal damage in a turbid medium," *Appl. Opt.* **36**, 32–43 (1997).
19. V. P. Zharov, S. G. Vesnin, S. E. Harms, J. Y. Suen, A. V. Vaisblat, and N. Tikhomirova, "Combined interstitial laser therapy for cancer using microwave radiometric sensor and RODEO MRI feedback," *Proc. SPIE* **4257**, 370–376 (2001).
20. V. P. Zharov, S. G. Vesnin, J. Y. Suan, and S. E. Harms, "Photothermal/microwave radiometry for imaging and temperature feedback," *Proc. SPIE* **4618** 324–333 (2002).
21. J. Kim, J. Oh, H. W. Kang, M. D. Feldman, and T. E. Milner, "Photothermal response of supermagnetic iron oxide nanoparticles," *Lasers Surg. Med.* **40**, 415–421 (2008).